

PROGRESS REVIEW • OPEN ACCESS

Recent progress of Na-flux method for GaN crystal growth

To cite this article: Yusuke Mori *et al* 2019 *Jpn. J. Appl. Phys.* **58** SC0803

View the [article online](#) for updates and enhancements.

You may also like

- [Reducing GaN crystal dislocations through lateral growth on uneven seed crystal surfaces using the Na-flux method](#)
Shogo Washida, Masayuki Imanishi, Ricksen Tandryo et al.
- [Progress in bulk GaN growth](#)
Ke Xu, , Jian-Feng Wang et al.
- [Suppression of newly generated threading dislocations at the regrowth interface of a GaN crystal by growth rate control in the Na-flux method](#)
Hyoga Yamauchi, Ricksen Tandryo, Takumi Yamada et al.



Recent progress of Na-flux method for GaN crystal growth

Yusuke Mori^{1*}, Masayuki Imanishi¹, Kosuke Murakami¹, and Masashi Yoshimura²

¹Graduate School of Engineering, Osaka University, 2-1 Yamadaoka, Suita, Osaka 565-871, Japan

²Institute of laser Engineering, Osaka University, 2-1 Yamadaoka, Suita, Osaka 565-871, Japan

*E-mail: mori.yusuke@eei.eng.osaka-u.ac.jp

Received February 4, 2019; accepted March 10, 2019; published online May 22, 2019

In this review, the history of research and development of the Na-flux method for growing single GaN crystals is summarized from its discovery in 1994 until the present. Underlying the development of the Na-flux method, which has become one of the more important technologies for growing high quality GaN crystals, there have been several important innovations without which it would have been impossible to achieve current technical levels. Here, we describe the development of the Na-flux method through these innovations, including a method for controlling nucleation by adding carbon, single- and multipoint seed techniques, and a hybrid of the flux-film coated and multipoint seed approaches.

© 2019 The Japan Society of Applied Physics

1. Introduction

Blue light-emitting diodes (LEDs) are fabricated through techniques involving the deposition of a buffer layer at a low temperature¹⁾ and p-type GaN crystals,²⁾ both of which were developed by Akasaki, Amano, and colleagues. Following these discoveries, GaN-based semiconductors have been used not only in LEDs but also in semiconductor lasers and high-frequency power electronic devices. To further enhance device performance, it is necessary to produce high-quality, low-cost bulk GaN crystals.

The high pressure solution growth (HPSG) method,³⁻⁵⁾ which was pioneered in Poland, has been used for many years to produce high quality bulk GaN crystals. However, the high pressure and temperature conditions (e.g., 10 000 atm and 1500 °C) required by the HPSG method make it difficult to achieve mass production of large-sized bulk GaN. In 1997, Ref. 6 proposed a Na-flux method in which GaN crystals can be grown in a Ga–Na mixed solution at relatively low pressures under a nitrogen (gas) atmosphere (<50 atm) and in a lower temperature range (700 °C–900 °C) than is required under the HPSG method. The Na-flux method has the advantage of enabling the synthesis of high-quality GaN crystals through spontaneous nucleation processes through the use of very simple equipment. During the initial stages of research, however, it proved difficult to grow large GaN crystals at a moderate growth rate as a result of difficulties in controlling the nucleation process. Nevertheless, significant advances have been made in the 25 years following the discovery of the Na-flux method, and it is currently possible to grow high-quality GaN crystals with diameters greater than two inches through the use of techniques involving the coalescence of GaN crystals from many isolated small seeds.

This article looks back at the research and development history of the Na-flux method from its discovery until the present. The Na-flux method has been evolving by the innovation of new technology. Therefore, in this article, we classify the Na-flux method into three stages. The first stage technology is normal liquid phase epitaxy (LPE) of GaN crystal on conventional GaN seed crystal so called “First

generation of Na-flux technique”. The second stage technology so called “second generation of Na-flux technique” consists of utilizing the multi-point seed technique (MPST). The third stage technology is the most advanced technology which has been discovered by hybridizing the MPST and the flux film coated (FFC) technique. We call this technology “third generation of Na-flux technique”. We will discuss the latest advancements associated with these techniques and their results.

2. Discovery of GaN crystal growth using Na-flux

From 1994 to 1995, Yamane, working at the research laboratory of F. J. DiSalvo at Cornell University, synthesized crystals of new ternary nitrides containing alkaline-earth metals by using Na-flux metal to clarify their crystal structures. To overcome the general inability of nitrogen to dissolve into a Na melt, Yamane added Zn to the melt. Because Zn forms a nitridometallate anion group, nitride synthesis could be carried out using the Ba–Zn–N system, producing nitride single crystals that were unstable in air and covered with Na. Using this method, ternary nitrides such as Sr₂ZnN₂, Ba₂ZnN₂, Ba₃Ga₂N₄, and Ba₅Si₂N₆, the oxynitride Ba₃ZnN₂O₂, and Ba₃Ge₂N₂, a compound containing nitridometallate anions and Zintl anions, were produced. In total, six new materials were synthesized.

Through an analysis of the new materials produced using this method, Yamane found that the use of Na is very effective in the synthesis of a number of ternary nitrides. He also became interested in the effects of Na on the synthesis of binary nitrides. Using Ga- and Si-based materials used to synthesize the ternary nitrides Ba₃Ga₂N₄ and Ba₅Si₂N₆, he attempted to prepare single binary nitride crystals by adding Na and NaN₃ to Ga. Following the experiment, tiny transparent crystals that were visible to the naked eye were found; X-ray diffraction measurement of these revealed that they were composed of GaN.^{6,7)} Although this achievement marked the moment of discovery of the Na-flux method, Yamane did not continue to fabricate GaN at Cornell out of a lack of interest because GaN was not a new compound. However, upon being informed of the value of his discovery upon returning to Japan, he then published an article on the



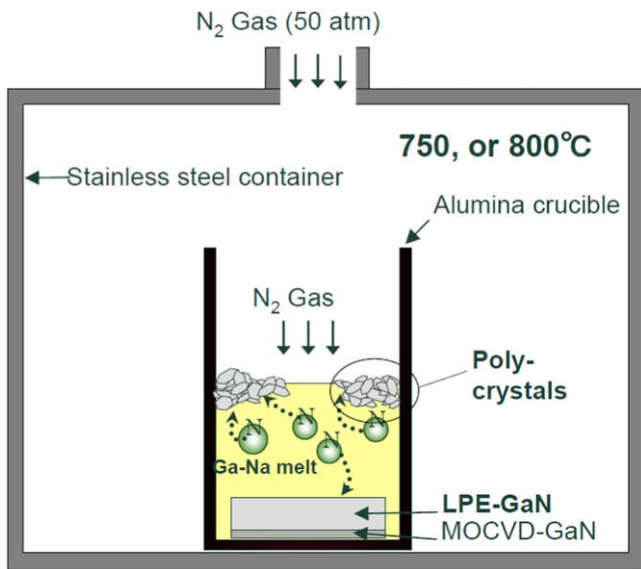


Fig. 1. (Color online) Schematic of GaN crystal growth via Na-flux method. Reprinted from Ref. 8 with permission from Elsevier.

Na-flux method and presented it at a conference. Upon hearing Yamane’s presentation at the Materials Research Society Meeting in 1996, the author of this paper (Y. Mori) decided to begin research on the Na-flux method.⁸⁾ Graciously, Yamane imparted all of his knowledge concerning the Na-flux method to him.

3. Discovery of carbon doping for nucleation control

Although the Na-flux method has significant advantages as a technique for synthesizing GaN crystals, the growth of large GaN crystals through spontaneous nucleation has proven to be difficult. This has led to the development of the vapor phase growth method, through which large-diameter GaN crystals can be grown from a fabricated seed substrate. In the Na-flux method, spontaneous nucleation occurs near the gas-liquid interface, as the concentration of nitrogen in this region is higher than at the bottom of the solution (Fig. 1).⁸⁾ This can hinder application of the vapor phase growth method because the spontaneous polycrystalline GaN crystal nucleation will tend to outpace the GaN crystal growth on a seed substrate located at the bottom of the solution.

Thus, preventing unfavorable nucleation is an important issue in solution growth because crystal quality and growth rate are limited by spontaneous nucleation. Fortunately, the authors discovered that doping carbon into the solution can significantly suppress spontaneous nucleation on areas other than the substrate.⁹⁾

Figure 2 shows the dependence of polycrystal and LPE yield on the amount of carbon additive at 750 °C and 800 °C.⁸⁾ The starting Ga:Na composition ratio was 27:73 mol%. Na (>3 N), which was shipped in Ar gas, was inserted in Ar-filled groove box (GB). In GB, the Na was set in a crucible after the oxide film removed. Graphite carbon (6N) was added in a crucible with Na and Ga. Nitrogen gas at 50 atm was introduced to increase nitrogen concentration in Ga–Na melt. Details such as equipment configuration or estimated nitrogen concentrations are described in Ref. 8. The vessel was allowed to cool naturally, and the crucible was then removed and immersed in cold ethanol and water to

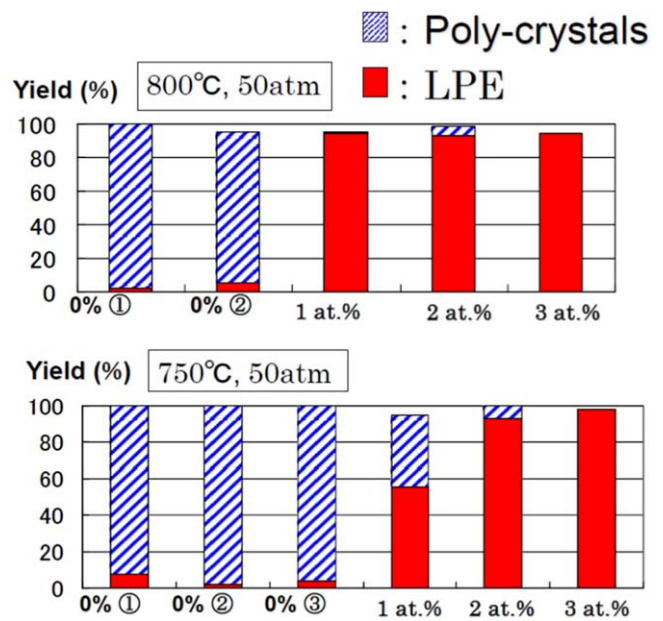


Fig. 2. (Color online) Dependence of LPE-GaN and polycrystal yield on addition of carbon at 750 °C and 800 °C. Reprinted from Ref. 8 with permission from Elsevier.

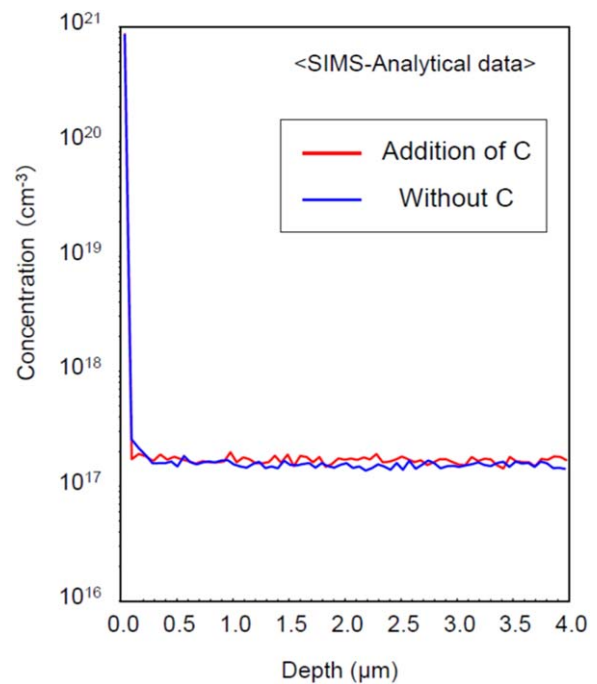


Fig. 3. (Color online) SIMS measurements of carbon concentrations in LPE crystals grown in a pure system and in a carbon-added system. Reprinted from Ref. 8 with permission from Elsevier.

dissolve the residual flux. At 800 °C and a carbon additive atomic percentage exceeding 1 at%, the generation of GaN polycrystals is completely eliminated. At 750 °C, an atomic percentage of 3 at% is required to completely eliminate GaN polycrystal generation, although the addition of carbon consistently reduces the level of polycrystal formation.

The higher carbon additive concentration required to eliminate polycrystals at the lower temperature appears to reflect the fact that there is a higher projected supersaturation level at 750 °C than at 800 °C. The mechanism for suppression of polycrystalline growth and the enhancement of

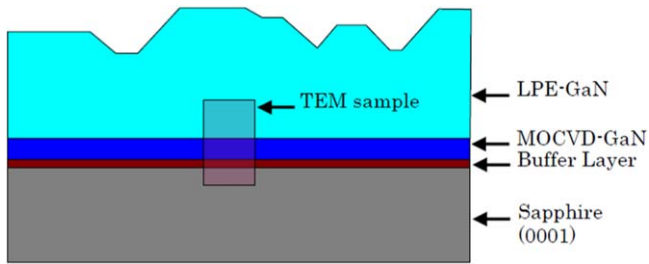


Fig. 4. (Color online) Schematic of GaN sample used for TEM observation. Reprinted from Ref. 8 with permission from Elsevier.

single-crystal growth was identified by systematically calculating activation free energies for the formation and dissociation of C–N bonds.¹⁰ Figure 3 shows carbon concentrations in LPE crystals grown with and without carbon.⁸ It is seen that the presence of carbon in the solution appears to have no bearing on the carbon concentration in the crystals; in both cases, the concentrations of carbon are low ($<10^{17} \text{ cm}^{-3}$).

4. LPE growth of GaN by the Na-flux method (“First generation of Na-flux technique”)

The suppression of spontaneous nucleation of GaN polycrystals by carbon doping makes it possible to grow GaN crystal on a seed crystal alone. The metal-organic chemical vapor deposition (MOCVD) and hydride vapor phase epitaxy (HVPE) methods can be used to prepare larger-diameter GaN seed crystals. Although a number of methods for reducing dislocation in GaN crystals, such as the epitaxial lateral over growth method, have been developed in conjunction with the MOCVD and HVPE methods, thus far they have proven incapable of producing sufficient crystallinity.^{11,12}

By contrast, the Na-flux method can be used to grow large GaN crystals with low dislocation density (on the order of 10^5 cm^{-2} on MOCVD-GaN thin film, which has a high

dislocation density of over 10^8 cm^{-2}).^{13–15} Transmission electron microscopy (TEM) observations of the interfaces between MOCVD-GaN and LPE-GaN have revealed that significant reductions in dislocation density occur in the initial stage of LPE growth. TEM observation has also shed light on the dislocation reduction mechanism. LPE-GaN crystals were grown on MOCVD-GaN film deposited on a sapphire (0001) substrate. A portion around the interface between the LPE-GaN and MOCVD-GaN was cut out, the sample was thinned to 200 nm using a focused ion beam, and a TEM (Hitachi H-800, accelerated voltage: 200 kV) was used to investigate the dislocation behavior (Fig. 4).⁸ A reflection vector of 11-22 was adopted to enable observation of various types of dislocation (Burgers vectors $b = \langle 0001 \rangle$, $1/3\langle 11-20 \rangle$, and $1/3\langle 11-23 \rangle$) in the sample and TEM images were captured via bright-field imaging under the Bragg condition.

Figure 5(a) shows a TEM [1-100] image of the LPE-GaN–MOCVD-GaN interface. During LPE growth, nearly all dislocations originating from the MOCVD-GaN disappeared within $2 \mu\text{m}$, with most of the dislocations becoming bent during the initial LPE growth stage and then concentrated as shown in Fig. 5(b).⁸ The TEM observations suggest that the number of dislocations were significantly reduced during LPE growth by application of the Na-flux method; this natural reduction in dislocation during growth is an excellent feature of the Na-flux approach that is not produced under other GaN crystal growth methods.

Stirring the solution during growth is an effective method for improving the quality of crystals grown using the Na-flux method¹⁶ because it enhances the morphology of the GaN crystals and increases their yields.¹⁷ A number of stirring methods can be used, including the application of a seesaw motion to the chamber to induce solution flow. The flow induced by the seesaw motion has a well-defined pattern and

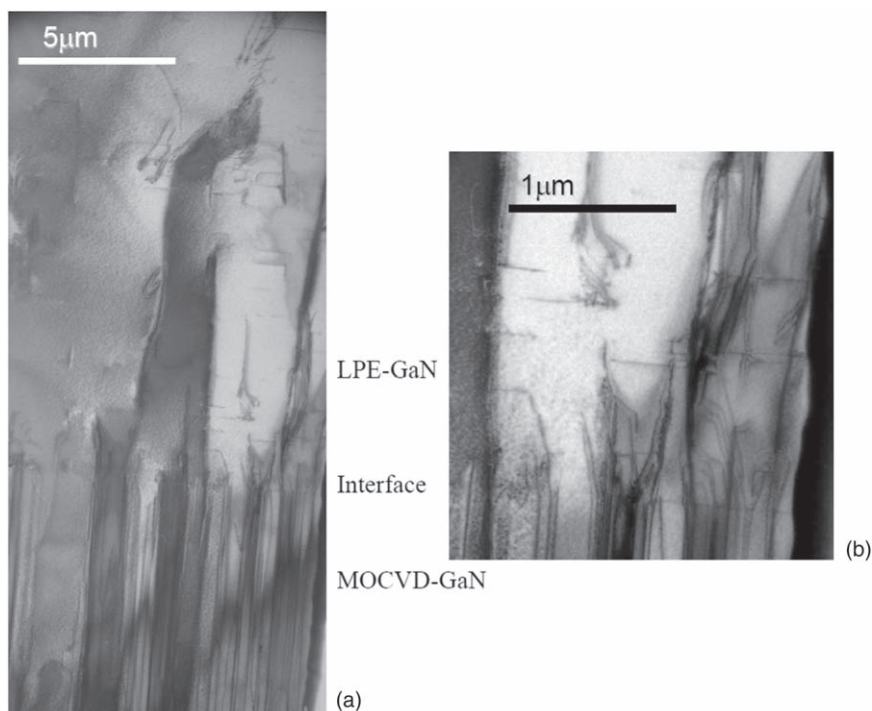


Fig. 5. (Color online) (a) TEM photograph of the interface between MOCVD-GaN and LPE-GaN. (b) Enlarged view of (a). Reprinted from Ref. 8 with permission from Elsevier.

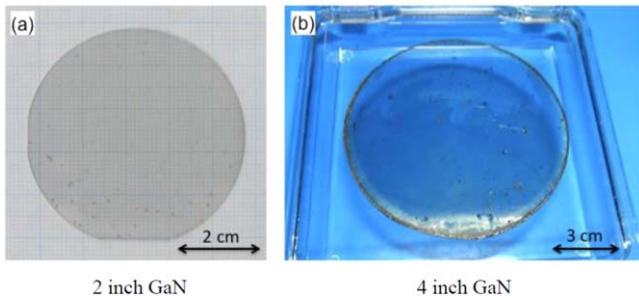


Fig. 6. (Color online) (a) Two- and (b) four-inch GaN crystals grown on HVPE-GaN crystals. Reprinted from Ref. 8 with permission from Elsevier.

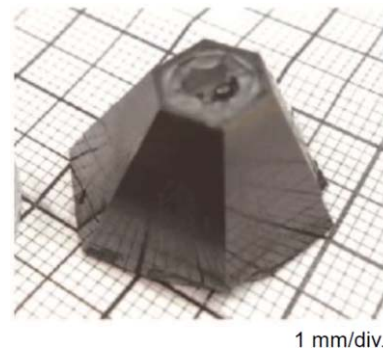


Fig. 9. (Color online) Optical photograph of bulk GaN crystal grown via single-point seed technique. Pyramid-shaped, well-faceted GaN single crystals can be grown over a period of 400 h.



Fig. 7. (Color online) Six-inch GaN crystal grown on MOCVD-GaN substrate using Na-flux method. Reprinted from Ref. 8 with permission from Elsevier.

can increase flow velocity to up to 2 cm s^{-1} , a factor 30 times higher than what is possible without the motion. The flatness of the grown GaN surface depends on the flow velocity and uniformity along the growing surface. As shown in Fig. 6, we were able to grow 2–4 in diameter GaN crystals with high uniformity and without cracks on an HVPE substrate.^{8,16} As shown in Fig. 7, it is also possible to grow 6 in diameter GaN crystal on a MOCVD-GaN substrate; we call this technique the “first generation of Na flux technique”.⁸ The thickness of these crystals was about $500 \mu\text{m}$, and their dislocation density was $10^4\text{--}10^6 \text{ cm}^{-2}$.^{18,19}

5. Point seed techniques

5.1. Single-point seed technique (SPST)

By using the Na-flux method to induce LPE growth in the manner described in the preceding section, it was possible to reduce the dislocation density from $\sim 10^8$ down to $10^4\text{--}10^6 \text{ cm}^{-2}$ per seed.^{18,19} However, these dislocation densities were still high, and it was quite difficult to reduce bows appearing in the grown GaN crystal as a result of the large bows produced in the seed crystals grown using the HVPE and MOCVD methods. In 2012, we developed the SPST to grow high quality GaN crystals.^{17,20,21}

The SPST procedure is shown in Fig. 8.²⁰ Figure 8(a) illustrates the production of the GaN point seed by mounting a $430 \mu\text{m}$ thick sapphire plate containing a small hole ($0.5\text{--}1.5 \text{ mm}$ in diameter) onto a $10 \mu\text{m}$ thick MOCVD-GaN film grown on sapphire substrate. As shown in Fig. 8(b), GaN crystals are grown through the hole on the GaN point seed. This configuration suppresses the propagation of dislocation in the early growth stage; details of the dislocation reduction mechanism are given in Ref. 20. The temperature and N_2 pressure in the tube were respectively maintained at $870 \text{ }^\circ\text{C}$ and $3.0\text{--}4.0 \text{ MPa}$. Figure 9 shows a typical bulk GaN crystal grown via SPST (SPST-GaN). Well-faceted bulk GaN crystals, composed of $\{10\bar{1}1\}$ planes, with diameters and heights of up to 2.1 and 1.2 cm, respectively, have been formed at growth rates of $52 \mu\text{m h}^{-1}$ in a -directions ($[10\bar{1}2]$ directions) and $30 \mu\text{m h}^{-1}$ in the c -direction. Panchromatic cathodoluminescence mapping measurements [Figs. 10(a) and 10(b)] of GaN samples sliced from SPST-GaN crystals

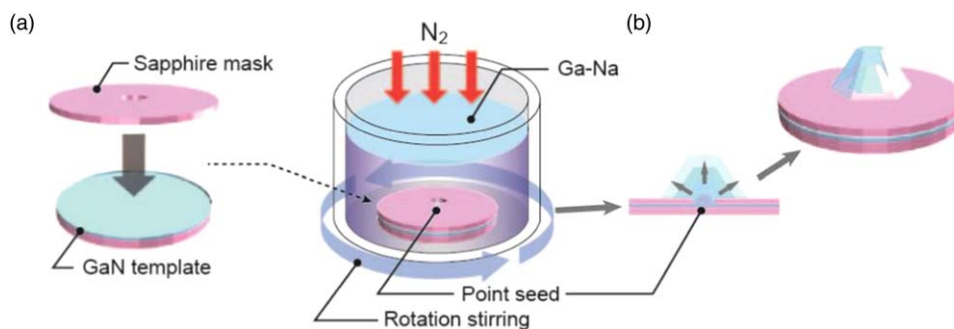


Fig. 8. (Color online) Schematic of experimental setup of single-point seed technique. (a) Configuration of GaN point seed produced by freely mounting a sapphire with a small hole onto a GaN template and placing it into a crucible with a diameter of 80 mm. The nitrogen source gas was pressurized at 50 atm during growth, and the solution was stirred by intermittently rotating the crucible. (b) Illustration of crystal growing on the point seed. The crystal grows through the small hole in the sapphire wafer. Reprinted from Ref. 8 with permission from Elsevier.

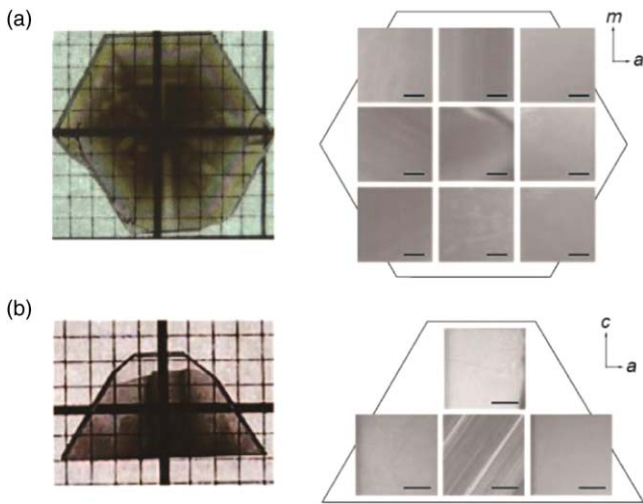


Fig. 10. (Color online) Photographs and panchromatic CL images of (a) *c*- and (b) *m*-face GaN samples sliced from bulk GaN crystal. Dark spots associated with dislocations could not be observed. Reprinted from Ref. 8 with permission from Elsevier.

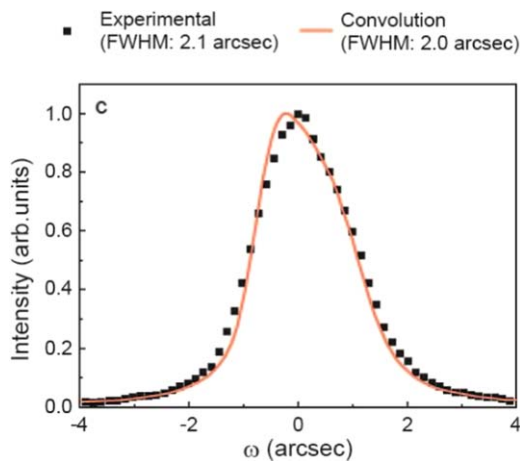


Fig. 11. (Color online) Experimental X-ray rocking curve (dotted line) of *c*-face GaN sample measured at the Spring-8 facility. The red curve shows the calculated XRC obtained by convoluting the X-ray beam and its theoretical (006) GaN. The experimental XRC and its FWHM (2.1 arcsec) are in close agreement with the calculated XRC (2.0 arcsec), indicating that the crystal structure is nearly perfect. Reprinted from Ref. 8 with permission from Elsevier.

have revealed *c*- and *m*-faces ($\{10\bar{1}0\}$ faces) that are nearly free of dislocations over their entire areas.²⁰⁾

The synchrotron X-ray beam produced at the BL24XU beamline at the SPring-8 facility was used to further evaluate the structural perfection of these GaN samples (details of the optical system used for this measurement are given in Ref. 22). The square symbols in Fig. 11 show the (006)

GaN X-ray rocking curve (XRC) obtained for the +*c*-face GaN sample. The FWHM value is 2.1 arcsec, which is nearly the same as in the simulated curve (FWHM: 2.0 arcsec, red curve in Fig. 11),²⁰⁾ indicating that this GaN crystal grown using the SPST has a nearly perfect structure. Although the SPST is effective at growing small to medium-sized high-quality GaN crystals, we found that it is not effective at growing large crystals. Accordingly, we sought to develop new technology for growing large high-quality GaN crystals.

5.2. MPST (“Second generation of Na flux technique”)

In 2013, we developed the MPST, which can be used to enlarge the diameter of the final GaN crystal by coalescence of smaller crystals grown from many isolated point seeds.^{23–25)} Figure 12 shows a schematic of the coalescence growth process. A multipoint seed GaN substrate (MPS-GaN sub.) is produced by patterning MOCVD-GaN films onto a sapphire substrate grown via MOVPE. Point seeds are then arranged in a hexagonal pattern. The point seed diameters and distances between the centers of neighboring seeds range from 0.25 to 1 mm and from 0.20 to 1 mm, respectively. The high-quality GaN crystals grown on each point seed can easily coalesce and unify during growth.

Figure 13 shows a photograph of a typical coalesced 2 in GaN crystal obtained via MPST. The sapphire substrate easily separated from the MPS-GaN sub.²⁵⁾ The XRC profiles of (0002) GaN and (10 $\bar{1}$ 2) GaN in Fig. 14 have FWHM values of 27.7–30.6 and 13.3–15.8 arcsec at (0002) and (10 $\bar{1}$ 2) diffraction, respectively.²⁵⁾

Figure 15 shows the results of mapping the XRC peak top angles for the GaN template (MOCVD-GaN film on sapphire substrate (solid circles)), MPS-GaN sub. (open circles), and coalesced GaN crystal (1.5 mm thick) after separation from the sapphire (solid squares).²⁵⁾ The radii of curvature correspond to the inverses of the slopes of the line in Fig. 15. The results reveal a large GaN template lattice curvature with a radius of 4.4 m but very little curvature for either the MPS-GaN sub. or coalesced GaN crystal (the >100 m radius of lattice curvature in both cases corresponds to the measuring limit of the X-ray diffractometer). Based on this transition in lattice curvature radius, the coalescence growth can be assumed to proceed as follows. First, the GaN template bends significantly owing to the difference between the thermal expansion coefficients of the GaN layer and the sapphire substrate. The strain caused by this difference in thermal expansion coefficient is eventually released when the GaN layer separates into a point-seeded shape as a result of the patterning. Finally, Na-flux coalescence growth on the low-curvature MPS-GaN sub. produces a low-curvature coalesced GaN crystal. Although distortion should occur as the temperature begins to fall following Na-flux

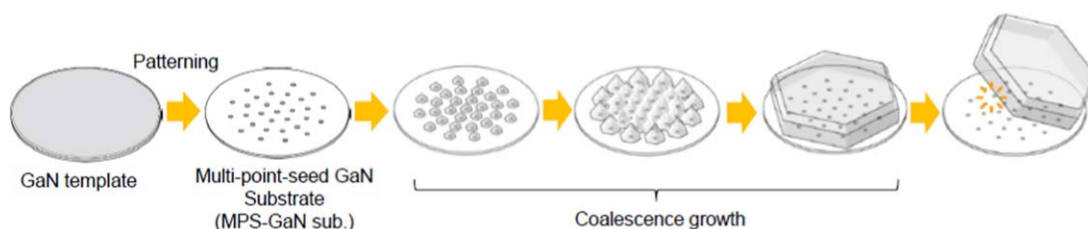


Fig. 12. (Color online) Schematic of coalescence growth process. A multipoint-seed-GaN substrate (MPS-GaN sub.) is produced by patterning a GaN film onto a sapphire substrate via MOVPE. High-quality GaN crystals grown on each point seed easily coalesce and unify during growth. Following growth, the coalesced GaN naturally separates from the sapphire substrate. Reprinted from Ref. 8 with permission from Elsevier.

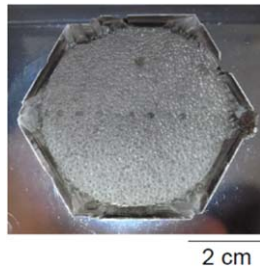


Fig. 13. (Color online) Photograph of 2 in GaN crystal grown via coalescence growth. GaN crystals grown from many point seeds have coalesced and unified during growth. The sapphire substrate easily separated from the MPS-GaN sub. following growth. Reprinted from Ref. 8 with permission from Elsevier.

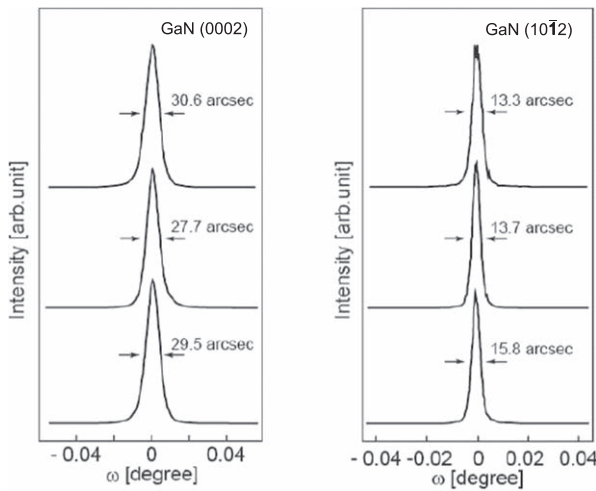


Fig. 14. (Color online) XRC measurement results for coalesced crystal, showing mapping profiles of (0002) and (10-12) GaN XRC. Reprinted from Ref. 8 with permission from Elsevier.

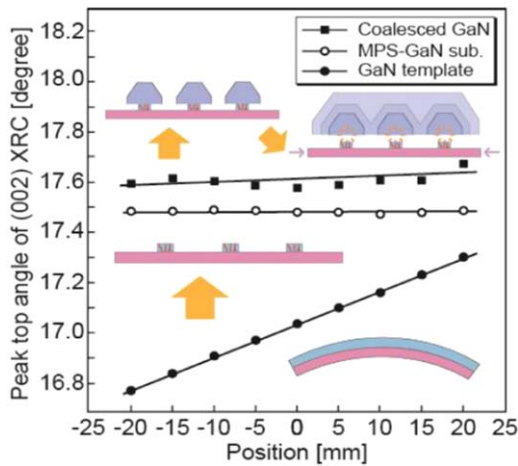


Fig. 15. (Color online) XRC peak top angle at various measurement points on different samples. The inverse slope of each line represents the radius of lattice curvature. The solid and open circles and solid squares represent the shifts in XRC peak top angle in the GaN template, MPS-GaN sub., and coalesced GaN crystal after separation from the sapphire substrate, respectively. Reprinted from Ref. 8 with permission from Elsevier.

growth as a result of the difference in thermal expansion coefficients between the coalesced crystal and the sapphire, the separation occurring immediately in the multipoint-seed areas as a result of the high detachability between the coalesced GaN

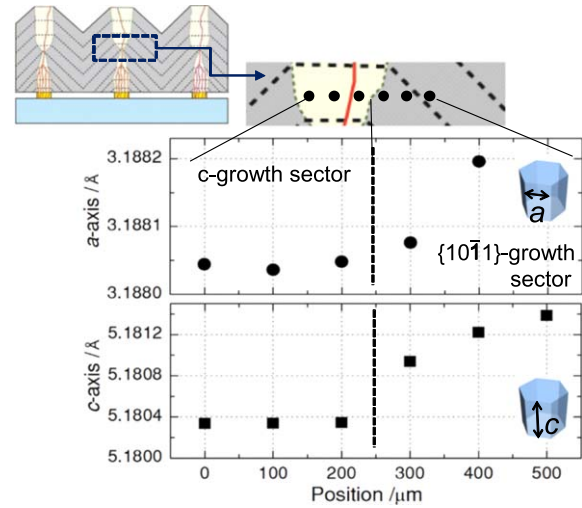


Fig. 16. (Color online) Lattice constants measured in *c*- and {10-11}-growth sectors.

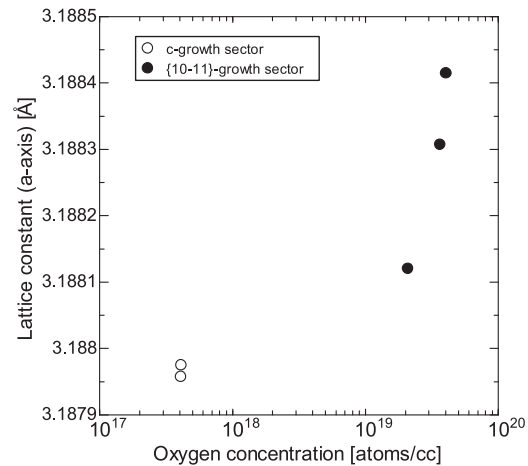


Fig. 17. (Color online) Relationship between lattice constant and oxygen concentration in *c*- and {10-11}-sectors.

crystal and the sapphire substrate causes the distortion to disappear.

We next focus on the blackness of SPST- and MPST-grown GaN crystals, as exemplified by the sample shown in Fig. 9. Based on a conjecture that the blackening is caused by oxygen impurities leading to expansion of lattice constants, as has been previously reported,²⁶ we carefully analyzed the lattice constants of several GaN crystals using the synchrotron X-ray beam produced at the BL24XU beamline of SPring-8. We found that the lattice constants in the *c*-growth sector were more uniform but smaller than those in the {10-11}-growth sector (Fig. 16).²⁷ A subsequent investigation of the relationship between oxygen concentration and crystal lattice constant revealed that the oxygen concentration in the {10-11}-sector was higher than in the *c*-growth sector and that the lattice constant along the *a*-axis expanded as the oxygen concentration increased, indicating that the crystal volume changed as a result of oxygen impurities (Fig. 17). The difference in oxygen concentration between growth sectors resulted in differences in coloration, as shown in Fig. 18.

These results suggest that an Na-flux wafer that is fully composed of *c*-growth sector material should have uniform

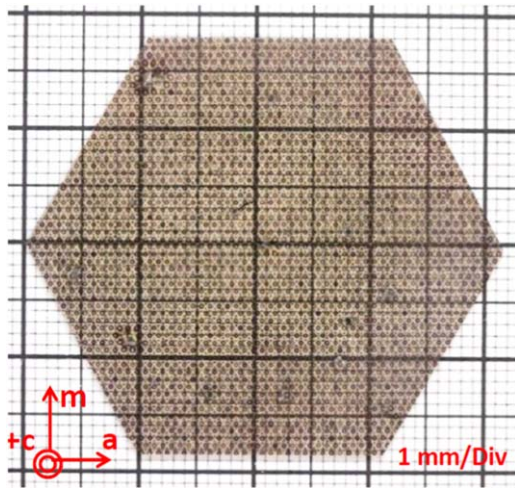


Fig. 18. (Color online) Photograph of 2 in GaN crystal grown via coalescence process in which GaN crystals are formed from the coalescence and unification of many point seeds. The sapphire substrate separated naturally from the MPS-GaN sub.

lattice constants. New technology to grow GaN crystal with uniform lattice constants is discussed in the next section.

6. FFC MPST (“Third generation of Na-flux technique”)

In the preceding section, we described the successful production of high-quality, large-diameter (>2 in) GaN crystals through the coupling of the MPST to the Na-flux method.²⁵⁾ However, the lattice constant of a GaN crystal grown via the MPST will change depending on the growth mode. In the pyramidal facets that appear in a crystal grown conventionally on a point seed,²⁸⁾ the oxygen concentration

will be enhanced relative to that in the *c*-plane growth sector.²⁷⁾ Thus, the production of uniform GaN crystals on a multipoint GaN sub. requires a crystal surface that is grown solely within a *c*-plane growth sector. Although a high-supersaturation growth condition can effectively enhance lateral growth and induce expansion along the *c*-plane,²⁹⁾ the growth habit cannot be changed significantly by simply altering supersaturation through the adjustment of parameters such as temperature or Ga–Na melt composition.³⁰⁾

To significantly enhance the supersaturation, we attempted to induce crystal growth in the thin flux film naturally formed by the residual Ga–Na melt around pyramidal GaN crystals following the extraction of MPS-GaN sub. from the melt in a crucible.³¹⁾ The thin flux film enables crystal growth at the high nitrogen concentrations constituting a high-supersaturation condition near the gas–liquid interface.³²⁾ This technique comprises a combination of the MPST and the FFC technique.⁹⁾ In previous iterations of the FFC technique, *c*-plane GaN grown via MOCVD on sapphire was used as a seed substrate to enable GaN crystal growth along a flat *c*-plane surface. However, the Ga–Na melt could not be retained on the surface following extraction of the substrate, resulting in growth discontinuation. Instead of growing GaN crystals on an MPS-GaN substrate composed of pyramidal {10 $\bar{1}$ 1}-plane facets with rough morphology, it should be possible to maintain the Ga–Na melt between the crystals and ensure continuous growth.

To attempt to initiate the new growth technique, we used the following procedure. First, the Ga–Na melt was prepared with the substrate kept outside the crucible until nitrogen supersaturation was reached, as shown in Fig. 19(a),³¹⁾ to prevent meltback of the point seeds.³³⁾ Upon supersaturation, the substrate was dipped in the melt, as shown in Fig. 19

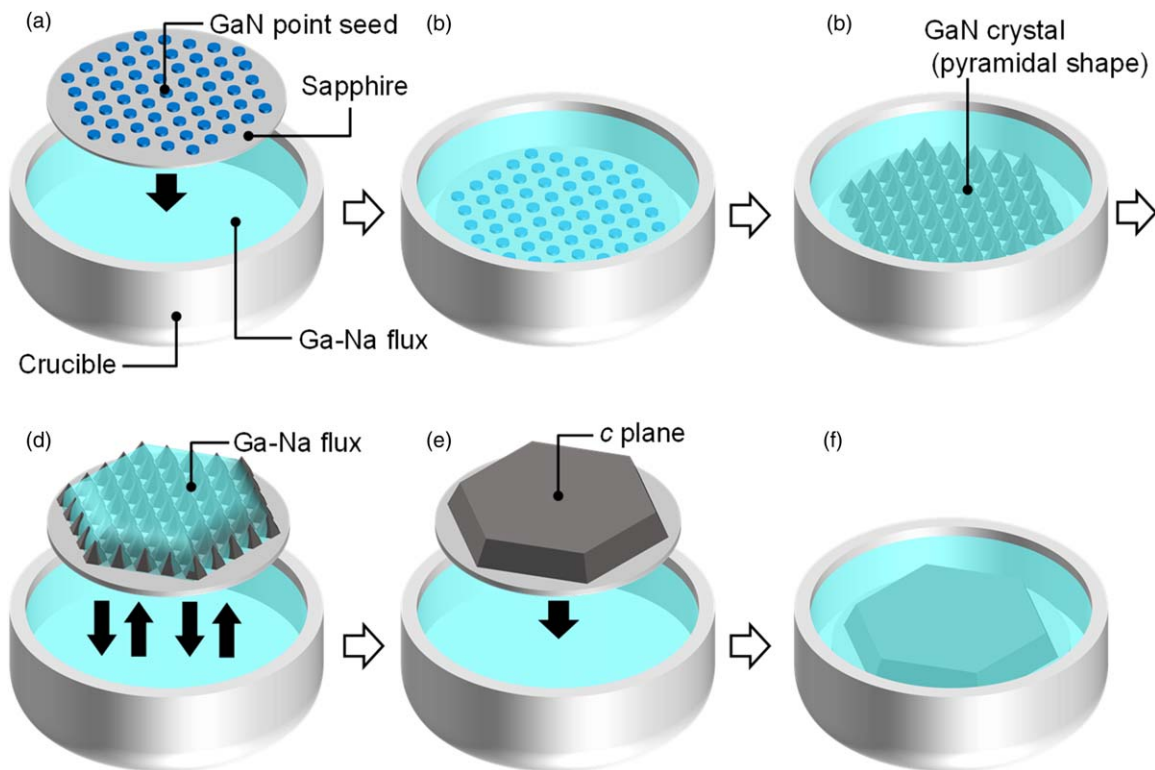


Fig. 19. (Color online) Schematics of surface flattening process. (a)–(c) show the conventional “first growth” called dipping technique. (d) shows the new flattening process using residual flux following extraction of the substrate (“second growth”). (e) and (f) show the final thick growth process (“third growth”).

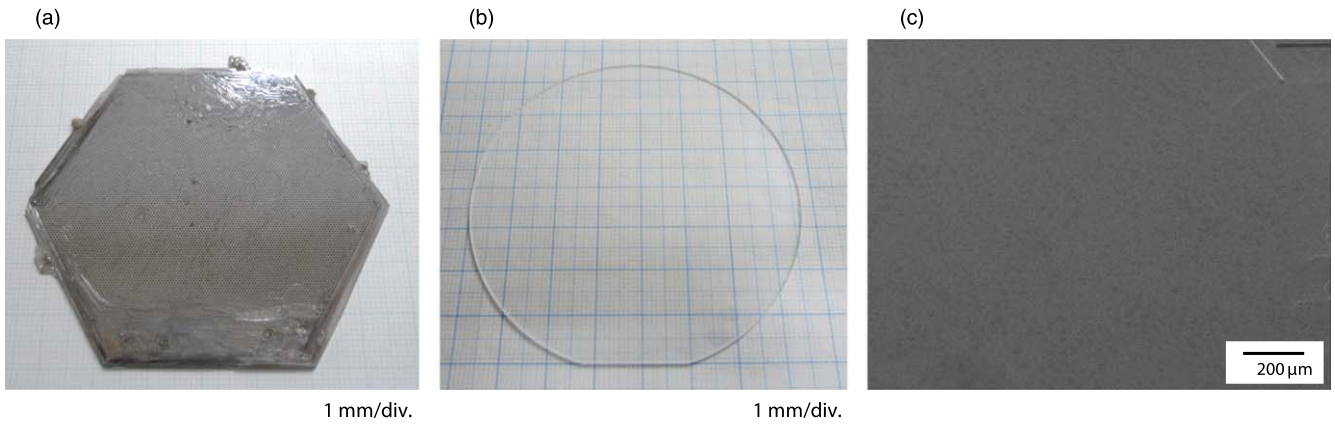


Fig. 20. (Color online) (a) Photo image of as-grown GaN wafer and (b) sapphire substrate from which the wafer naturally separated during the cooling process. (c) Surface bird's-eye SEM image of the wafer.

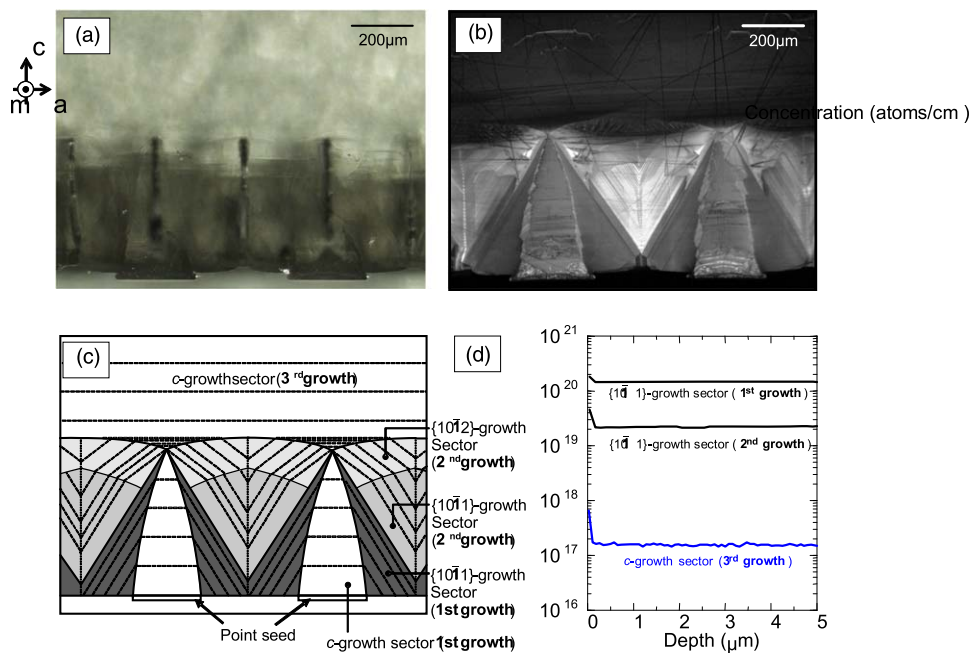


Fig. 21. (Color online) Cross-sectional (a) optical microscope and (b) CL images and corresponding schematic of an area grown from two-point seeds. (d) shows the measured SIMS depth profiles in the {10 $\bar{1}$ 1}, {10 $\bar{1}$ 2}, and *c*-growth sectors.

(b),³¹⁾ which induced the GaN crystals to begin to grow on the individual point seeds in the “first growth” [Fig. 19(c)].³¹⁾ The surfaces of the first-growth GaN crystals were composed of {10 $\bar{1}$ 1}-plane pyramidal facets.²⁸⁾ The substrate was then extracted from the Ga–Na melt [Fig. 19(d)] to form a residual flux between the GaN crystals that enabled growth across a thin-flux film.³¹⁾ However, because there was an insufficient amount of Ga in the thin flux, growth could not continue. To correct this, we supplied Ga to the thin flux by repeatedly dipping the substrate into the Ga–Na melt in the crucible at specific intervals in what we called the “second growth” process. Following second growth, which produced pure flat *c*-plane crystal surfaces [Fig. 19(e)],³¹⁾ the substrate was dipped again into the Ga–Na melt in the crucible, as shown in Fig. 19(f),³¹⁾ to increase the thickness of the *c*-plane growth sector in the “third growth” process.

Figure 20(a) shows a photograph of as-grown GaN crystal obtained using the new technique.³¹⁾ During the cooling process, the sapphire substrate naturally separated from the crystal wafer without the generation of cracks, as shown in



Fig. 22. (Color online) Free-standing GaN wafer with a high transparency and 2 in diameter obtained following backgrounding of the first- and second-growth sectors and the application of a chemical mechanical polishing process.

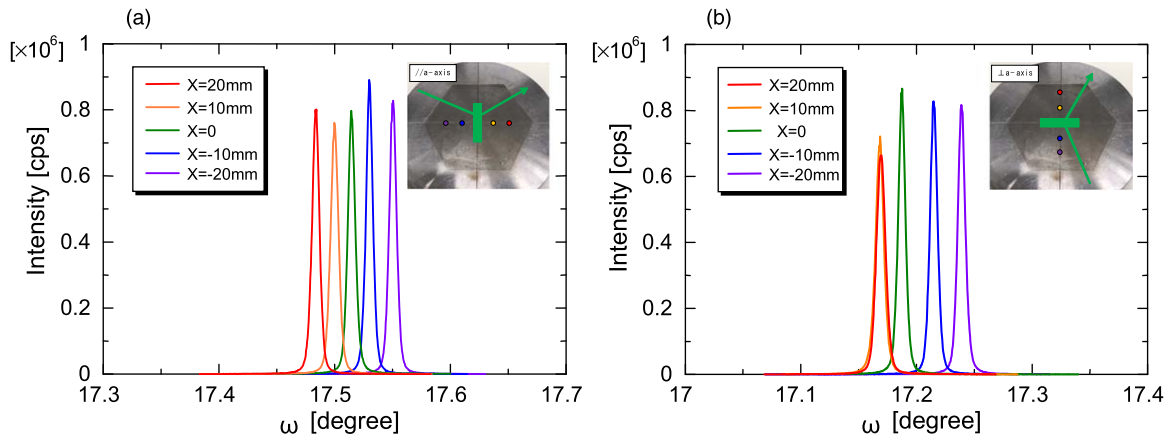


Fig. 23. (Color online) On-axis GaN (0002) ω -XRCs obtained from X-ray beams parallel to the (a) a (all) and (b) m (mll) directions. Five measurements were taken over 10 mm steps along each incident X-ray direction.

Fig. 20(b),³¹⁾ and a crack-free GaN wafer with a flat c -plane surface [Fig. 20(c)] was obtained following third growth.³¹⁾ Figure 21(a) shows an optical microscope image of a cross-section of GaN crystal at an area grown from two-point seeds.³¹⁾ The first- and second-growth sectors are black, while the third-growth sector is colorless and highly transparent. Figures 21(b) and 21(c) show,³¹⁾ respectively, a panchromatic CL image and a schematic of the same position. Although the crystal formed following first (conventional) growth had a rough surface composed of $\{10\bar{1}1\}$ -plane pyramidal facets, a completely flat surface comprising a c -plane was obtained after the second growth. The flatness of the second-growth crystal was retained during the third growth. Figure 21(d) shows SIMS depth profiles of each growth sector.³¹⁾ The average oxygen concentrations at depths of 2–5 μm were 1.5×10^{20} , 2.2×10^{19} , and 1.5×10^{17} atoms cm^{-3} in the first-, second-, and third-growth sectors, respectively. Through this process, a GaN layer with a low oxygen concentration could be obtained, which enabled good lattice matching with HVPE GaN crystals. By backgrounding the first- and second-growth sectors and applying a chemical mechanical polishing process, a free-standing GaN wafer with high transparency and a diameter greater than two inches was successfully obtained, as shown in Fig. 22.³¹⁾

We then evaluated the structural quality of the wafer in terms of the FWHM of the XRC. Figures 23(a) and 23(b) show on-axis GaN (0002) ω -XRCs produced by X-ray beams incident along the a (all) and the m (mll) directions, respectively.³¹⁾ All the XRCs exhibit a single peak. The FWHM values are as narrow as 24–29 and 25–33 arcsec for all for mll , respectively, indicating an extremely high crystallinity and uniformity across the entire surface of the sample. The radii of curvature for all and mll are 30 and 33 m, respectively, while those of the as-grown wafer prior to grinding of its backside were 16 and 22 m for all and mll , respectively. We believe that the lattice bowing was caused by lattice mismatch between the third- and the first- and second-growth sectors, in which the lattice constants expanded owing to high oxygen concentrations. Following elimination of the first- and second-growth sectors, the bowing was reduced.

Threading dislocation density was measured from the dark-spot density over a 170 μm square area of two-photon

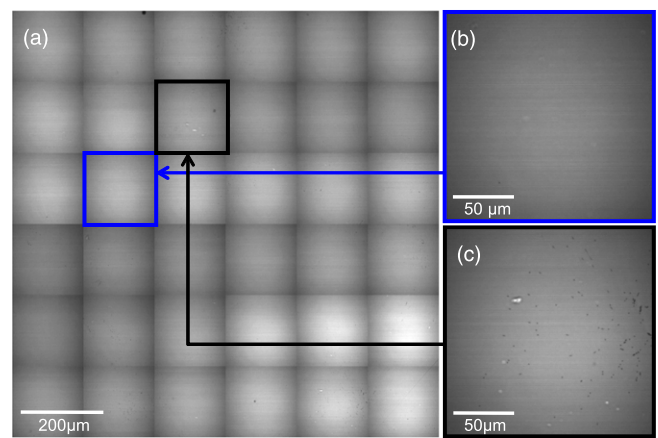


Fig. 24. (Color online) (a) 170 μm square area of 2PPL images with a mapping of 6×6 points, with magnified images of (b) lowest- and (c) highest-dislocation density areas.

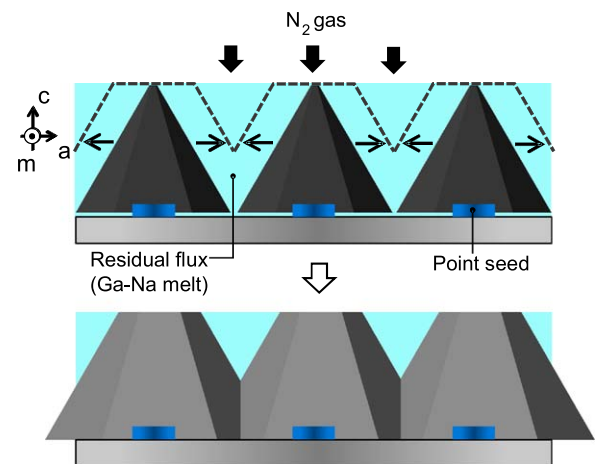


Fig. 25. (Color online) Schematic of surface flattening process by residual flux between pyramidal GaN crystals formed by extracting the MPS-GaN substrate during the second growth.

excitation photoluminescence images with a mapping of 6×6 points [Fig. 24(a)].³¹⁾ The lowest dislocation density was $3.5 \times 10^3 \text{ cm}^{-2}$ [Fig. 24(b)], while the highest was $4.4 \times 10^5 \text{ cm}^{-2}$ [Fig. 24(c)].³¹⁾ These observation areas contain the layer formed by the coalescence of GaN crystals grown from four-point seeds during the second growth

process. In other words, coalescence boundaries, which can be considered high-dislocation density areas, were included in all of these areas, enabling us to estimate the dislocation density over the entire region to be on the order of 10^3 – 10^5 cm⁻².

Finally, we discuss the mechanism of surface flattening by the residual flux, as illustrated in Fig. 25.³¹⁾ We propose two mechanisms for the flattening. First, it is possible that the low flux level allows for growth in Ga–Na melts with high nitrogen concentrations near the gas–liquid interface, a mechanism that has been reported to promote lateral growth.²⁹⁾ The high concentrations of nitrogen can be explained by the lower oxygen concentrations in the second-growth sector relative to the first-growth sector, as shown in Fig. 21(d), which occurs as a result of the previously reported³⁴⁾ lack of oxygen incorporation in the nitrogen-rich condition. The second potential mechanism is that residual flux is present only around the pyramidal GaN crystals, which would restrict growth to the lateral direction because crystals can grow only in the Ga–Na melt. Once the surface becomes a completely flat *c*-plane following the second growth, it is difficult for the flux to remain on the surface owing to the poor flux wettability on the *c*-plane, resulting in the cessation of crystal growth. Thus, the first growth process is important in that it allows for the retention of a thin flux around the pyramidal facets, while the third growth process allows for the thickening of the *c*-growth sector at low oxygen concentrations. GaN crystals obtained using the new proposed technique would be expected to demonstrate good lattice matching with HVPE GaN crystals, which would enable rapid and thick growth on a wafer and the formation of large-diameter bulk GaN crystals with low dislocation density.

7. Summary

In this paper, recent progress in the Na-flux method for inducing GaN crystal growth was discussed. Significant results have been reported during the 25 years since the discovery of the Na-flux method, and the third generation of Na-flux technique, which builds upon preceding innovations, can enable the growth of large-diameter, low-bow, high-quality GaN crystals, opening a new door to the development of low-cost, high-performance GaN-based electronic and optoelectronic devices.

- 1) H. Amano, N. Sawaki, I. Akasaki, and Y. Toyoda, *Appl. Phys. Lett.* **48**, 353 (1986).
- 2) H. Amano, M. Kito, K. Hiramatsu, and I. Akasaki, *Jpn. J. Appl. Phys.* **28**, L2112 (1989).
- 3) S. Porowski, *J. Cryst. Growth* **166**, 583 (1996).
- 4) S. Porowski and I. Grzegory, *J. Cryst. Growth* **178**, 174 (1997).

- 5) J. Karpinski, J. Jun, and S. Porowski, *J. Cryst. Growth* **66**, 1 (1984).
- 6) H. Yamane, M. Shimada, S. J. Clarke, and F. J. DiSalvo, *Chem. Mater.* **9**, 413 (1997).
- 7) H. Yamane, *J. Ceram. Soc. Jpn.* **117**, 7 (2009).
- 8) Y. Mori, M. Imade, M. Maruyama, M. Yoshimura, H. Yamane, F. Kawamura, and T. Kawamura, in *Handbook of Crystal Growth: Bulk Crystal Growth: Basic Techniques*, ed. P. Rudolph (Elsevier, Amsterdam, 2015) 2nd ed., p. 505.
- 9) F. Kawamura, M. Morishita, M. Tanpo, M. Imade, M. Yoshimura, Y. Kitaoka, Y. Mori, and T. Sasaki, *J. Cryst. Growth* **310**, 3946 (2008).
- 10) T. Kawamura, H. Imabayashi, M. Maruyama, M. Imade, M. Yoshimura, Y. Mori, and Y. Morikawa, *Appl. Phys. Express* **9**, 015601 (2015).
- 11) A. Usui, H. Sunakawa, A. Sakai, and A. Yamaguchi, *Jpn. J. Appl. Phys.* **36**, L899 (1997).
- 12) K. Hiramatsu, K. Nishiyama, M. Onishi, H. Mizutani, M. Narukawa, A. Motogaito, H. Miyake, Y. Iyechika, and T. Maeda, *J. Cryst. Growth* **221**, 11 (2000).
- 13) F. Kawamura, T. Iwahashi, K. Omae, M. Morishita, M. Yoshimura, Y. Mori, and T. Sasaki, *Jpn. J. Appl. Phys.* **42**, L4 (2003).
- 14) F. Kawamura, T. Iwahashi, M. Morishita, K. Omae, M. Yoshimura, Y. Mori, and T. Sasaki, *Jpn. J. Appl. Phys.* **42**, L729 (2003).
- 15) M. Morishita, F. Kawamura, M. Kawahara, M. Yoshimura, Y. Mori, and T. Sasaki, *J. Cryst. Growth* **270**, 402 (2004).
- 16) Y. Mori et al., *J. Cryst. Growth* **350**, 72 (2012).
- 17) K. Murakami, D. Matsuo, H. Imabayashi, H. Takazawa, Y. Todoroki, A. Kitamoto, M. Maruyama, M. Imade, M. Yoshimura, and Y. Mori, *Jpn. J. Appl. Phys.* **52**, 08JA03 (2013).
- 18) M. Imade, Y. Hirabayashi, Y. Konishi, H. Ukegawa, N. Miyoshi, M. Yoshimura, T. Sasaki, Y. Kitaoka, and Y. Mori, *Appl. Phys. Express* **3**, 075501 (2010).
- 19) F. Kawamura, M. Tanpo, N. Miyoshi, M. Imade, M. Yoshimura, Y. Mori, Y. Kitaoka, and T. Sasaki, *J. Cryst. Growth* **311**, 3019 (2009).
- 20) M. Imade, K. Murakami, D. Matsuo, H. Imabayashi, H. Takazawa, Y. Todoroki, A. Kitamoto, M. Maruyama, M. Yoshimura, and Y. Mori, *Cryst. Growth Des.* **12**, 3799 (2012).
- 21) M. Imade, M. Maruyama, M. Yoshimura, and Y. Mori, *Jpn. J. Appl. Phys.* **53**, 05FA06-1 (2014).
- 22) S. Takeda, K. Yokoyama, Y. Tsusaka, Y. Kagoshima, J. Matsui, and A. Ogura, *J. Synchrotron Radiat.* **13**, 373 (2006).
- 23) M. Imanishi, K. Murakami, H. Imabayashi, H. Takazawa, Y. Todoroki, D. Matsuo, M. Maruyama, M. Imade, M. Yoshimura, and Y. Mori, *Appl. Phys. Express* **5**, 095501 (2012).
- 24) M. Imanishi, K. Murakami, H. Imabayashi, H. Takazawa, Y. Todoroki, D. Matsuo, M. Maruyama, M. Imade, M. Yoshimura, and Y. Mori, *Phys. Status Solidi C* **10**, 400 (2013).
- 25) M. Imade et al., *Appl. Phys. Express* **7**, 035503 (2014).
- 26) C. G. Van de Walle, *Phys. Rev. B* **68**, 165209 (2003).
- 27) M. Imanishi, Y. Todoroki, H. Murakami, D. Matsuo, H. Imabayashi, H. Takazawa, M. Maruyama, M. Imade, M. Yoshimura, and Y. Mori, *J. Cryst. Growth* **427**, 87 (2015).
- 28) M. Imanishi, T. Yoshida, T. Kitamura, K. Murakami, M. Imade, M. Yoshimura, M. Shibata, Y. Tsusaka, J. Matsui, and Y. Mori, *Cryst. Growth Des.* **17**, 1806 (2017).
- 29) H. Yamane et al., *Jpn. J. Appl. Phys.* **44**, 3157 (2005).
- 30) M. Honjo, M. Imanishi, H. Imabayashi, K. Nakamura, K. Murakami, D. Matsuo, M. Maruyama, M. Imade, M. Yoshimura, and Y. Mori, *Opt. Mater.* **65**, 38 (2017).
- 31) M. Imanishi, K. Murakami, T. Yamada, K. Kakinouchi, K. Nakamura, T. Kitamura, K. Okumura, M. Yoshimura, and Y. Mori, *Appl. Phys. Express* **12**, 045508-1 (2019).
- 32) F. Kawamura, M. Morishita, K. Omae, M. Yoshimura, Y. Mori, and T. Sasaki, *Jpn. J. Appl. Phys.* **42**, L879 (2003).
- 33) T. Sato et al., *Jpn. J. Appl. Phys.* **54**, 105501 (2015).
- 34) A. F. Wright, *J. Appl. Phys.* **98**, 103531 (2005).